Microplastic atmospheric dustfall pollution in urban environment: Evidence from the types, distribution, and probable sources in Beijing, China

Pengju Liu[1], Longyi Shao[1]*, Yaowei Li[1,2], Tim Jones[3], Yaxin Cao[1], Cheng-Xue Yang[4], Mengyuan Zhang[1], M. Santosh[5,6], Xiaolei Feng[1], Kelly BéruBé[7]

1. State Key Laboratory of Coal Resources and Safe Mining & College of Geoscience and Surveying Engineering, China University of Mining and Technology (Beijing), Beijing 100083, China
2. Hebei Center for Ecological and Environmental Geology Research, Hebei GEO University, Shijiazhuang 050031, China
3. School of Earth and Environmental Sciences, Cardiff University, Cardiff, CF10, 3YE, Wales, UK
4. Institute of Earth Sciences, China University of Geosciences (Beijing), Beijing 100083, China
5. School of Earth Sciences and Resources, China University of Geoscience Beijing, Beijing 100083, China
6. Department of Earth Science, University of Adelaide, Adelaide, SA 5005, Australia
7. School of Biosciences, Cardiff University, Cardiff CF10 3AX, Wales, UK

The corresponding author is Longyi Shao
E-mail: ShaoL@cumtb.edu.cn

21 Graphical Abstract

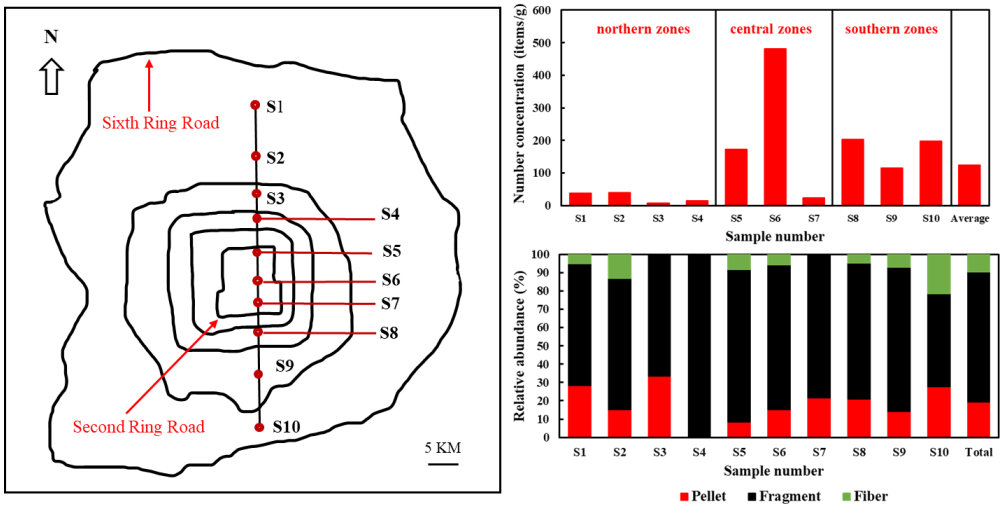

22

23

Highlights:

1. Microplastic pollution in the central Beijing is more serious than in the northern and southern zones.
2. Nine different compositions of microplastics were identified with polypropylene being the most abundant.
3. The morphologies of microplastics include fragments, pellets, and fibers; with fragments being the most common.
4. The presence of aged microplastics was recorded in the dustfall samples.

Abstract

Airborne microplastics (MPs) pollution is an environmental problem of increasing concern, due to the ubiquity, persistence and potential toxicity of plastics in the atmosphere. In recent years, most studies on MPs have focused on aquatic and sedimentary environments, but little research has been done on MPs in the urban atmosphere. In this study, a total of ten dustfall samples were collected in a transect from north to south across urban Beijing. The compositions, morphologies, and sizes of the MPs in these dustfall samples were determined by means of Laser Direct Infrared (LDIR) imaging and Field Emission Scanning Electron Microscopy (FESEM). The number concentrations of MPs in the Beijing dustfall samples show an average of 123.6 items/g. The MPs concentrations show different patterns in the central, southern, and northern zones of Beijing. The number concentration of MPs was the highest in the central zone (224.76 items/g), as compared with the southern zone (170.55 items/g), and the northern zone (24.42 items/g). The LDIR analysis revealed nine compositional types of MPs, including Polypropylene (PP), Polyamide (PA), Polystyrene (PS), Polyethylene (PE), Polyethylene Terephthalate (PET), Silicone, Polycarbonate (PC), Polyurethane (PU) and Polyvinylchloride (PVC), among which PP was overall dominant. The PP dominates the MPs in the central zone (76.3%), and the PA dominates the MPs in the southern zone (55.86%), while the northern zone had a diverse combination of MPs types. The morphological types of the individual MPs particle include fragments, pellets, and fibers, among which fragments are dominant (70.9%). FESEM images show the presence of aged MPs in the Beijing atmosphere, which could pose a yet unquantified health risk to Beijing's residents. The average size of the MPs in the Beijing samples is 66.62 μm. Our study revealed that the numbers of fibrous MPs increase with the decrease in size. This pollution therefore needs to be carefully monitored, and methods of decreasing the sources and mitigations developed.

Keywords: Microplastics, LDIR, FESEM, chemical composition, morphology, health risk

1. Introduction

Microplastics (MPs), as an entirely anthropogenic type of pollution, are considered to be stratigraphic markers of the Anthropocene Epoch (Corcoran et al., 2018). MPs are plastics with small particle sizes, usually less than 5 mm (Arthur et al., 2009, Shao et al., 2022a), that originate from both primary and secondary sources (Cole et al., 2011, Shao et al., 2022a). Primary MPs are mainly sourced from common commercial products that contain microscopic plastics as part of their manufacture; such as personal care, cosmetics, cleaning, and medical products (Wang et al., 2019). Secondary MPs originate from the environmental degradation of larger-sized plastic products (Akhbarizadeh et al., 2017). Plastic is widely used in numerous fields, including packaging, construction, automotive, textile, medical, electronic, agriculture, sports, and safety equipment (Andrady, 2011; Brahney et al.. 2020; Gallagher et al.. 2016; Mohammadizadeh et al.. 2019). Plastic has advantages that include low price, lightweight, strength, practicality, and durability (Moore, 2008). Since the 1950s, approximately 8300 million metric tons of plastics have been manufactured worldwide (Geyer et al., 2017). By 2025, the accumulation of plastic in the environment could reach 11 billion tons (Brahney et al., 2020). As the demand for plastics continues to grow, the rate of accumulation of MPs in the environment has increased dramatically (Serranti et al., 2018). MPs pollution is rapidly becoming a pressing global issue, which has attracted commercial, environmental and public concern.

The accumulation of MPs in the environment can potentially exacerbate ecosystems and increase health risks (Kvale et al., 2021). Although water treatment plants can reduce the concentration of MPs

in wastewater by up to 98%, large volume of MPs are still discharged into the receiving waters every day (Murphy et al., 2016). Large amounts of MPs can be ingested by marine organisms with non-selective filter-feeding behavior (Wang et al., 2021). In the scientific literature, MPs have been detected in fish (Ding et al., 2018), shellfish (Ding et al., 2020), bivalves (Van Cauwenberghe and Janssen, 2014), and earthworms (Jiang et al., 2020). Studies have confirmed that MPs can affect the feeding, multiple molting, reproduction, growth, mortality, immune responses, and oxidative stress of marine organisms (Bergami et al., 2016; Devriese et al., 2015; Jeong and Choi, 2019; Limonta et al., 2019; Qiao et al., 2019, Ward and Kach, 2009; Zhang et al., 2021b). MPs are by definition very small and therefore have a relatively large specific surface area; especially after aging and crushing (Mao et al., 2020). A large specific surface area and hydrophobic characteristics make MPs more susceptible to adsorption of toxic and hazardous substances, such as polycyclic aromatic hydrocarbons (PAHs) (Klasios et al., 2021), organochlorine pesticides (OCPs) (Zhang et al., 2021a), polychlorinated biphenyls (PCBs) (Pastorino et al., 2021) and heavy metals (e.g., Cd, Pb, Cr, Cu, Zn) (Guo and Wang, 2021). Aged MPs can adsorb toxic and harmful substances, thus posing a potential threat to the human body. The possible dangers posed by MPs on ecosystems and human health needs to be better understood.

Recently, most research on MPs has focused on different aquatic environments such as rivers, groundwater, lakes, and seawater (Bharath et al., 2021; Clayer et al., 2021; Kooi et al., 2021; Woodward et al., 2021), and sedimentary environments such as island sediments, terrestrial, river, and marine sediments (Braun et al., 2021; Saarni et al.,2021; Vermeiren et al., 2021; Yan et al., 2021; Zhou et al., 2021). In addition, there are also studies on long-distance MPs transport. The studies found that MPs can be transported to remote areas mostly unaffected by human influence, such as the Tibetan Plateau (Liang et al., 2022), Arctic (Hamilton et al., 2021), Himalayas (Yang et al., 2021) and

western Italian Alps (Parolini et al., 2021).

In spite of the increasing studies on MPs, there is still a paucity of research on atmospheric MPs, especially in megacities. MPs are recognized as widespread atmospheric pollutants due to their small sizes and low densities (Revell et al., 2021). The distributions and characteristics of MPs in cities and their influencing factors are still unclear. Due to limitations of available analytical techniques, there is little information about the variations of concentrations, particle sizes and morphologies of MPs in the atmosphere.

In this study, MPs in ten atmospheric dustfall samples were studied to elucidate the pollution role of MPs in Beijing atmosphere. The morphological characteristics and compositional types of MPs, and the regional distribution characteristics of MPs within Beijing were investigated. The variations in the number concentrations, particle sizes, and morphologies of MPs within the atmosphere are considered. The results of this study provide new insights into particulate pollution compositions in the urban atmosphere of megacities.

2. Materials and methods

2.1. Sample collection

Samples were collected in urban areas of Beijing, China (Fig. 1). To understand the distribution of MPs in the atmosphere, ten sampling sites were selected and the samples were collected at 2-7 km intervals in a transect from the northern to the southern areas of the city. The atmospheric dustfall was mostly collected on a smooth surface (non-plastic component). To minimize contamination, the atmospheric dustfall was collected with an antistatic brush and dustpan, using a brush type that minimizes potential brush fiber contamination. The bulk samples were stored in a sealed aluminum

foil bag. The collection data detailing the local environment of the sampling sites, and wind direction is shown in Table 1.

Separated by the Second Ring Road, the sampling sites are divided into three zones (Fig 1). The northern zone refers to the northern area outside of the northern Second Ring Road, including S1, S2, S3 and S4. The central zone refers the area within the Second Ring Road, including S5, S6, and S7. The southern zone refers to the southern area outside of the southern Second Ring Road, including S8, S9, and S10.

2.2. MPs separation

In this study, $ZnCl_2$ solution was used as heavy-liquid to separate MPs by density flotation from the bulk samples, which predominantly consisted of denser mineral particles. Previous research has shown that this method is effective (Bellasi et al., 2021; Liu et al., 2019b; Shao et al., 2022a). The steps are: (1) configure 1.7-1.8 $g \cdot cm^{-3}$ $ZnCl_2$ (premium pure) solution; (2) place a measured amount of atmospheric fallout bulk dust into a 100 mL beaker, add 60 mL $ZnCl_2$ solution, stir the mixture for two minutes, and then allow to stand over 72 hours; (3) transfer the surface floating component to another beaker and add 60 mL of 30% H_2O_2 to digest the organic matter, which includes agitating it on an oscillator for 10 min, and then standing for 24 hours to allow the H_2O_2 to fully digest the organic matter; (4) MPs are collected by vacuum extraction filtration using a filter membrane (silver membrane with a pore size of 0.45 μm), and then placed in a sterile petri dish for air-drying (5) place the dried filter in ethanol and extract the sample off the filter into the solution, aided by ultrasound; (6) remove the filter membrane from the ethanol and wash with ethanol several times until the filter is clean, The ethanol was allowed to evaporate down to a volume of 200 μL, then a drop of the ethanol is put on a glass coverslip. Once the ethanol has completely evaporated leaving the sample adhered

to the glass surface the samples are prepared for FESEM and LDIR analysis.

2.3. FESEM analysis

The projected image of the plastic particles provided by the LDIR imaging system is not clear, and the size is larger than 20 μm. Therefore, FESEM was used to observe the microscopic characteristics of the MPs (Li et al., 2020b). Studies have shown that FESEM is a very effective method for the characterization of atmospheric particles (Shao et al., 2022a, Shao et al., 2022b). The FESEM used in this study was a SUPRA 40 (Zeiss Germany) based at Henan Normal University. The prepared sample on the glass coverslip was placed on the stub using conductive double-sided tape and gold coated. The FESEM analysis was under 20 KV voltage and the working distance was less than 5 mm.

2.4. LDIR analysis

The LDIR (Agilent 8700) analyzer was used to characterize the types and sizes of MPs. The LDIR uses a Quantum Cascade Laser (QCL) as the light source, which has over 10,000 times the energy of traditional Fourier Transform infrared (FT-IR) spectroscopy. The collimating laser accurately aligns the light rays and directly irradiates the sample after optical path conversion (Li et al., 2021). Even for micron-scale samples the infrared spectrum has a sufficient signal-to-noise ratio to achieve accurate chemical characterization. Previous studies have confirmed that the LDIR Analyzer is an advanced and reliable method for detecting plastics (Li et al., 2021; Ng et al., 2021). In this study, fast single-wavelength (1800 cm^{-1}) light can scan the MPs on the slide, and the image analysis software can measure the MPs sizes >20 μm. Once the MPs were located, the LDIR automatically moved around to scan particles on the slide, and the infrared median range spectrum of

each particle was collected, and compared with the standards in a plastics reference library (Li et al., 2021). To ensure the reliability of the identification, only the results with a matching degree greater than or equal to 0.8 were selected.

3. Results

3.1. MPs number concentrations

MPs were detected in all the samples. The number concentration in this study refers to the number of MPs particles (items) per gram of dustfall. The abundance of MPs at all the sample sites ranged from 7.25 items/g to 481.39 items/g, with an average of 123.6 items/g. The highest number concentration of MPs was found at the sampling site S6, at 481.39 items/g, followed by S8 (202.29 items/g), S10 (197.03 items/g), S5 (172.73 items/g), S9 (115.19 items/g), S2 (38.85 items/g), S1 (37.62 items/g), S7 (22.95 items/g), S4 (13.64 items/g), and S3 (7.25 items/g) (Fig. 2).

The MPs distribution in the northern zone (S1, S2, S3, and S4), central zone (S5, S6, and S7), and southern zone (S8, S9, and S10) show different patterns. In the northern zone, the average number concentration was 24.42 items/g, in the central zone, the average number concentration was 224.76 items/g, and in the southern zone, the average number concentration was 170.55 items/g. The central zone has the highest average concentration of MPs, 1.3 times that of the southern zone and 9.2 times that of the northern zone. In the central zone, S5 was collected in Nanluoguxiang (South Luogu Lane) with street food stalls, a developed fast-food service and a high population density. The S6 sample site is in the center of the city, close to the world cultural heritage site the Forbidden City and shopping centers. There are also many service sectors such as catering, hotels, and shops around the S6 sampling site. The number concentration of MPs at the S7 sampling site was only 22.95 items/g, and

this low concentration may be due to that the sampling site is not in a residential area and has not been affected by road traffic (There are tall buildings between the sampling site and the road). The average number concentration of MPs in the southern zone was nearly seven times higher than in the northern zone. Sampling site S9 with the lowest number concentration (115.19 items/g) in the southern zone was higher than that at the S2 with the highest number concentration (38.85 items/g) in the northern zone (Fig. 2). In the northern zone, there are no other sources of MP pollution other than MPs created by the residents. Construction, traffic levels, and industries in the southern zone may be an important reason for the higher MPs number concentration in the southern zone compared to the northern zone. It appears that areas with high human activity levels will produce relatively higher number concentrations of MPs.

3.2. MPs chemical types

In our study, nine chemical types were recognized by LDIR, including Polypropylene (PP), Polyamide (PA), Polystyrene (PS), Polyethylene (PE), Polyethylene Terephthalate (PET), Silicone, Polycarbonate (PC), Polyurethane (PU) and Polyvinylchloride (PVC) (Fig. 3). The total samples statistics reveal the relative abundances of different types of MPs. The PP and PA were the major types, accounting for 56 items/g and 28.83 items/g respectively, followed by PE (8.82 items/g), PVC (8.48 items/g), PS (7.46 items/g), PET (5.67 items/g), PU (4.81 items/g), Silicone (3.05 items/g), and PC (0.48 items/g) (Fig. 4).

Our study found that the central, southern, and northern zones have different patterns in the relative proportions of the different compositional types of MPs. In the central zone, PP was the dominant component, accounting for 76.3%. In the southern zone, PA was the main component, accounting for 58.86%, followed by PS (15.08%) and PE (7.36%). In the northern zone, PP was again

the dominant component at 32.4%, followed by PA (18.1%), PE (17.05%), PET (11.92%), and Silicone (9.42%) (Fig. 5). Therefore, PP was the major contributor to the MPs pollution in the central and northern zones, whereas PA was the main component of MPs pollution in the southern zone. In the northern zone, MPs pollution consisted of diverse types of MPs.

3.3. MPs morphological types

Three morphological types of MPs were observed in this study: pellets/spheres (Fig. 6a), fragments (Fig. 6b), and fibers (Fig. 6c). Pellet/Sphere refers to the morphology of individual MPs with a rounded morphology. Fragment describes the morphology of individual MPs that are neither rounded or fibers. Fiber describes the morphology of individual MPs that have a length: width aspect ratio greater than 3. The fragments were the most common in all the sample sites. The number statistics for all samples were fragments (70.9%), followed by pellets/spheres (19.53%) and fibers (9.57%) (Fig. 7).

The study also identified that different chemical compositional types of MPs display different morphologies. PS had fragment and fiber morphologies, but no pellet/spheres, whereas PC was mostly pellets/spheres (Fig. 8). There was no apparent difference in the relative proportions of the different MPs morphological types in the central, southern, and northern zones of Beijing.

3.4. MPs size distributions

The size of the individual MPs particle in the Beijing samples ranged from 37.7 μm to 95.78 μm, with an average of 66.62 μm (Fig. 9). Different compositional types of MPs had different average sizes, with the PC being 95.78 μm, PP 78.08 μm, PET 69.7 μm, PE 63.23 μm, PS 66.18 μm, PVC 56.35 μm, PA 52.15 μm, PU 38.42 μm and Silicone 37.7 μm in descending order.

The size distributions are also different, with the average size of MPs in the central zone as 59.3 μm. In the southern zone, the average size of MPs is 57.52 μm. In the northern area, the average size of MPs is 70.67 μm. It is noted that the higher number concentrations of MPs were associated with the smaller average sizes in the central and southern zone.

We divided the size of MPs into three segments, 20-100 μm, 100-200 μm, and >200 μm. The study found that MPs accounted for 84.63%, 13.34% and 2.83% in size range 20-100 μm, 100-200 μm and >200 μm (Fig. 10) respectively. The results showed that the number concentration of MPs in the atmosphere increases with the decrease of size, with smaller MPs being associated with higher number concentration. The greater abundance of MPs in smaller sizes may be attributed to the rapid degradation of small plastic fragments (Zhang et al., 2016). In the >200 μm size segment, fibrous MPs accounted for 5.26%. In the 100-200 μm size segment, fibrous MPs accounted for 8.16%, and in the 20-100 μm size segment, fibrous MPs accounted for 10.39% (Fig. 11). The results indicate that the amounts of fibrous MPs in the atmosphere increases with the decrease of size. We also found that pellet/sphere, fragment, and fiber MPs are dominant in the 20-100 μm size segment (Fig. 12). These results indicate that the MPs in the atmosphere of Beijing mainly come from the degradation of large plastics.

4. Discussion

4.1. MPs aging and health risk

The aging processes and resulting MPs characteristics have been the subject of scientific investigation (Lambert and Wagner, 2016). The formation of aged MPs is part of the processes that will eventually lead to the breakdown of the plastics in the environment into non-plastic end products.

(Liu et al., 2019a). This degradation process can involve environmental weathering, ultraviolet radiation, biodegradation, physical wear and chemical oxidation (Jahnke et al., 2017). MPs can age more rapidly in the atmosphere than in water because of the availability of oxygen and higher levels of ultraviolet radiation (Mao et al., 2020). The temperature, ultraviolet rays, ozone and other substances in the atmosphere will directly act on MPs, resulting in their aging. In the Beijing dustfall samples, we found that many of the MPs have undergone various degrees of recognizable aging. Visual damage in the form of collapses, cracks, and structural embrittlement were observed in the FESEM images of some MPs (Fig. 6).

A study of remote lakeshore sediments on the Tibet Plateau found that damage to MPs might have resulted from collision with wind-mobilized sand grains (Zhang et al., 2016). Mineral particles are common in Beijing's atmosphere (Wang et al., 2022). It is speculated that many of the damage features seen at a microscopic level could have been the result of impact with atmospheric mineral particles. However, cracking and embrittlement may not be the result of just mechanical weathering, but the damage is likely to be a combination of ultraviolet radiation, oxidation, as well as the physical weathering. As stated, a significant proportion of the MPs are secondary particles derived from larger plastic pieces. Therefore, the regular observation of microscopic damage features is to be expected as part of the process of converting the primary sources into secondary particles. As the particles become smaller, the mechanisms of weathering are likely to subtly change as the smaller particles are less prone to physical assault and become more brittle. Once the particles become exceedingly small it is likely that most of the weathering damage is no longer physical, but rather driven by ultraviolet radiation and atmospheric oxidation.

Ultraviolet radiation and oxidation are important factors that cause carbon-carbon bond breaks in MPs as part of the plastic degradation process (Gewert et al., 2015). This change of chemical structure

and morphology will alter their macroscopic properties, with subsequent weathering leading to further embrittlement and disintegration of plastics (Halle et al., 2017). A study on the degradation of PS found that the size, surface morphology and microstructure will change with aging (Lambert and Wagner, 2016). The aging processes are generally believed to be capable of enhancing the sorption potential of MPs in soil, and mobility of the particles in groundwater (Ren et al., 2021). An isothermal adsorption model shows that aging can significantly increase the adsorption of heavy metals by PS (Mao et al., 2020).

In recent years, Beijing has experienced frequent haze events, and this atmospheric particulate matter contains a large number of harmful substances (Feng et al., 2020; Li et al., 2020a; Shao et al., 2021a). The dustfall samples have shown that the Beijing atmosphere contains MPs, which are part of the pollution cocktail. Human exposure to toxic substances can be through three different pathways: dermal, ingestion and inhalation (Cabral-Pinto et al., 2020). Dermal exposure is highly unlikely to present a health risk as the MPs levels are so low, and the skin presents an effective barrier to the MPs. Nanoparticles can cross the skin barrier, however the particles sizes recorded in this study are much larger than nanoparticles. It is however possible that some atmospheric MPs could exist as nanoparticles. Inhalation again depends upon the particle size, with $PM_{2.5}$ (aerodynamic diameter less than or equal to 2.5 μm) commonly considered to be the size that determines whether the particles are capable of being respired into the deep lung (Shao et al., 2022b). The smallest of the MPs types, Silicone, had an average size of 37.7 μm, and therefore is much larger than what is normally considered to be the largest atmospheric particulate matter PM_{10} (10 μm equivalent spherical diameter). In this case the silicone particles would be considered to be a nuisance dust, which would be filtered-out in the nose and upper airways. However, we also find MPs smaller than 2.5 μm (Fig. 6a) in this study. Although we cannot determine the type of MPs, these MPs have the same

297 aerodynamic characteristics as $PM_{2.5}$ particles in the air, and they can reach deep lungs or alveoli
298 through respiration (Enyoh et al., 2019). The most recent research has found MPs in human blood
299 (Leslie et al. 2022). In the third potential pathway airborne MPs can be inadvertently ingested, causing
300 physical damage to the body. Study have found that MPs can be absorbed by human tissues through
301 phagocytosis and cell adsorption in the respiratory system and gastrointestinal tract, leading to
302 inflammation, cell necrosis and tissue tearing (Enyoh et al., 2019). Research has shown that MPs can
303 bioaccumulate by ingestion in a range of organisms (Prata et al., 2020), typically organisms such as
304 aquatic filter-feeders. Airborne MPs can also enter the body by eating contaminated food (Khalid et
305 al., 2020). Furthermore, recent study has found that Novel Coronavirus can be transmitted by aerosols
306 (Shao et al., 2021b) and can survive on the surface of aerosols for up to 72 hours (Salimi et al. 2022).
307 MPs are also a kind of particulate matter in the atmosphere, so MPs may also be used as a viral carrier.
308 Based on the above discussion, we recognize that aged MPs in the Beijing atmosphere may adsorb
309 toxic and harmful substances. Smaller MPs of undetermined component types in the study (Fig. 6b)
310 may form part of $PM_{2.5}$, therefore, MPs with smaller sizes could pose a yet unquantified health risk
311 to Beijing's residents.

312 **4.2. MPs possible original sources: proximal and distal**

313 The compositions and morphologies of MPs are controlled by the chemistry of the original
314 plastics that were used in their manufactured sources. In this study, PP accounted for the highest
315 concentration in MPs, and the central Beijing zone has a highest level. The size of the particles and
316 their distribution across Beijing supports the view that a significant proportion of these MPs were
317 created in central Beijing. In the central zone, numerous service industries produce large number of
318 packaging products, such as foam plastic boxes, PP plastic cups, food packaging bags and other

similar products; these when degraded are likely to be an important component of PP aggregation at the S5 and S6 sample sites. In addition, PP is widely used in injection molded products (Li et al., 2018), so injection molded domestic products may also be a source of PP. The overall second highest number concentration and proportion of MPs is PA in the dustfall samples, with southern zone having the highest number concentration. PA plastics are often found as fibers that are mixed with other types of fibers to improve the wear resistance of fabrics (Liu et al., 2019b). With the breakdown or daily wear of those fabrics the individual PA fibres would be released as MPs (Wright et al., 2020). Research into indoor air at schools in Barcelona, Spain, has shown that the children's daily wear of clothing releases fibers into the school rooms, therefore this type of fibrous MP would be expected in any dense urban environment (Moreno et al., 2014). Investigations have shown that PA is widely used in many fields, including industries such as pharmaceutical, beverage, furniture, domestic machinery, transport, and clothing (Kasal et al., 2020; Welle et al., 2012). Since these industries are found in the southern zone, this area may be an important original source of PA. Given the distribution of the MPs within Beijing, their specific chemistries, and the probable original plastic sources, we can conclude that a significant percentage of the MPs are created locally from daily life, service industries and industrial emissions. Many of the waste plastic products will have been disposed of at ground level and disintegrated at that level by a combination of chemical and physical degradation. It is probable that a significant component of the dustfall MPs did not become sufficiently airborne to be inhalable but were moved around at a near surface level either by natural wind or anthropomorphic generated air movements, such as traffic air turbulence resuspension.

The morphologies of MPs provide important characteristics for tracing their possible sources. Fragments are the dominant morphological type of MPs in the Beijing dustfall. Previous studies have suggested that the fragmental MPs were created by the degradation of larger plastic objects (Müller

et al., 2018). The FESEM images show that larger fibrous MPs could splinter to create many more fibrous fragments with smaller particle sizes as a result of aging (Fig. 6d). The pellets or spheres MPs are generally thought to be primary particles released from personal care products, such as medicines, and cosmetics (Alidoust et al., 2021). Routinely used in cosmetics these MPs have a number of trade names, such micro-pearls, and nano-pearls, and given their microscopic size an individual application of skin cream can contain many tens of thousands of particles, available for release into the environment as the creams dry or are exposed to wind. As one of the largest megacities in the world, Beijing has a huge population, a developed economy and advanced medical technology. This vast population uses many medicines and applies MP-containing cosmetics on a daily basis, and this will be a significant source of the pellet/sphere MPs found in the Beijing dustfall.

5. Conclusions

1) The number concentrations of MPs in the Beijing dustfall show an average of 123.6 items/g, with the highest number being in the central zone, and the lowest number being in the northern zone.

2) Nine compositional types of MPs were identified in the Beijing dustfall, including PP, PA, PS, PE, PET, Silicone, PC, PU and PVC. PA is the most common plastic type in the southern zone, PP dominates the central zone, whereas the northern zone had a diverse combination of different compositional types.

3) The morphologies of the MPs in the Beijing dustfall are of three basic types: fragments, fibers, and pellet/spheres, with the fragments being the most common. There is no obvious distribution difference in the morphological types of MPs in the central, southern, and northern zone of Beijing. SEM images show the presence of aged MPs in the Beijing dustfall.

4) The average size of the MPs in the Beijing dustfall is 66.62 μm. The numbers of fibrous MPs

in the dustfall increases with the decrease of size. The results indicated that the MPs in the Beijing dustfall mainly come from the degradation of larger plastics.

6. Acknowledgments

This study is supported by the National Natural Science Foundation of China (Grant No. 42075107), the Fundamental Research Funds for the Central Universities (2022YJSDC05) and the Yueqi Scholar fund of China University of Mining and Technology (Beijing).

References

Akhbarizadeh, R., Moore, F., Keshavarzi, B. and Moeinpour, A., 2017. Microplastics and potentially toxic elements in coastal sediments of Iran's main oil terminal (Khark Island). Environmental Pollution 220, 720-731. http://doi.org/ 10.1016/j.envpol.2016.10.038

Alidoust, M., Yeo, G.B., Mizukawa, K. and Takada, H., 2021. Monitoring of polycyclic aromatic hydrocarbons, hopanes, and polychlorinated biphenyls in the Persian Gulf in plastic resin pellets. Marine Pollution Bulletin 165, 112052. http://doi.org/ 10.1016/j.marpolbul.2021.112052

Andrady, A.L., 2011. Microplastics in the marine environment. Marine Pollution Bulletin 62(8), 1596-1605. http://doi.org/ 10.1016/j.marpolbul.2011.05.030

Arthur, C., Baker, J., Bamford, H., Barnea, N. and Mcelwee, K., 2009. Summary of the international research workshop on the occurrence, effects, and fate of microplastic marine debris. In: Conference Proceedings, 9–11.

Bellasi, A., Binda, G., Pozzi, A., Boldrocchi, G. and Bettinetti, R., 2021. The extraction of microplastics from sediments: An overview of existing methods and the proposal of a new and green

alternative. Chemosphere 278, 130357. http://doi.org/ 10.1016/j.chemosphere.2021.130357

Bergami, E., Bocci, E., Vannuccini, M.L., Monopoli, M., Salvati, A., Dawson, K.A. and Corsi, I., 2016. Nano-sized polystyrene affects feeding, behavior and physiology of brine shrimp Artemia franciscana larvae. Ecotoxicology and Environmental Safety 123, 18-25. http://doi.org/ 10.1016/j.ecoenv.2015.09.021

Bharath, K.M., Natesan, U., Vaikunth, R., Kumar, R.P., Ruthra, R. and Srinivasalu, S., 2021. Spatial distribution of microplastic concentration around landfill sites and its potential risk on groundwater. Chemosphere 277, 130263. http://doi.org/ 10.1016/j.chemosphere.2021.130263

Brahney, J., Hallerud, M., Heim, E., Hahnenberger, M. and Sukumaran, S., 2020. Plastic rain in protected areas of the United States. Science 368(6496), 1257-1260. http://doi.org/ 10.1126/science.aaz5819

Braun, M., Mail, M., Heyse, R. and Amelung, W., 2021. Plastic in compost: Prevalence and potential input into agricultural and horticultural soils. Science of the Total Environment 760, 143335. http://doi.org/ 10.1016/j.scitotenv.2020.143335

Cabral-Pinto, M.M.S., Inacio, M., Neves, O., Almeida, A.A., Pinto, E., Oliveiros, B. and Ferreira da Silva, E.A., 2020. Human health risk assessment due to agricultural activities and crop consumption in the surroundings of an industrial area. Exposure and Health 12(4), 629-640. http://doi.org/ 10.1007/s12403-019-00323-x.

Clayer, F., Jartun, M., Buenaventura, N.T., Guerrero, J.-L. and Lusher, A., 2021. Bypass of Booming Inputs of Urban and Sludge-Derived Microplastics in a Large Nordic Lake. Environmental Science & Technology 55(12), 7949-7958. http://doi.org/ 10.1021/acs.est.0c08443

Cole, M., Lindeque, P., Halsband, C. and Galloway, T.S., 2011. Microplastics as contaminants in the marine environment: A review. Marine Pollution Bulletin 62(12), 2588-2597. http://doi.org/

10.1016/j.marpolbul.2011.09.025

Devriese, L.I., van der Meulen, M.D., Maes, T., Bekaert, K., Paul-Pont, I., Frère, L., Robbens, J. and Vethaak, A.D., 2015. Microplastic contamination in brown shrimp (Crangon crangon, Linnaeus 1758) from coastal waters of the Southern North Sea and Channel area. Marine Pollution Bulletin 98(1), 179-187. http://doi.org/ 10.1016/j.marpolbul.2015.06.051

Ding, J., Li, J., Sun, C., Jiang, F., He, C., Zhang, M., Ju, P. and Ding, N.X., 2020. An examination of the occurrence and potential risks of microplastics across various shellfish. Science of the Total Environment 739, 139887. http://doi.org/ 10.1016/j.scitotenv.2020.139887

Ding, J., Zhang, S., Razanajatovo, R.M., Zou, H. and Zhu, W., 2018. Accumulation, tissue distribution, and biochemical effects of polystyrene microplastics in the freshwater fish red tilapia (Oreochromis niloticus). Environmental Pollution 238, 1-9. http://doi.org/ 10.1016/j.envpol.2018.03.001

Enyoh, C.E., Verla, A.W., Verla, E.N., Ibe, F.C., Amaobi, C.E., 2019. Airborne microplastics: a review study on method for analysis, occurrence, movement and risks. Environ Monit Assess. 191 (11), 1–17. https://doi.org/10.1007/s10661-019-7842-0.

Feng, X.L., Shao, L.Y., Xi, C.X., Jones, T., Zhang, D.Z. and BeruBe, K., 2020. Particle-induced oxidative damage by indoor size-segregated particulate matter from coal-burning homes in the Xuanwei lung cancer epidemic area, Yunnan Province, China. Chemosphere 256, 127058. http://doi.org/ 10.1016/j.chemosphere.2020.127058

Gallagher, A., Rees, A., Rowe, R., Stevens, J. and Wright, P., 2016. Microplastics in the Solent estuarine complex, UK: An initial assessment. Marine Pollution Bulletin 102(2), 243-249. http://doi.org/ 10.1016/j.marpolbul.2015.04.002

Gewert, B., Plassmann, M.M. and MacLeod, M., 2015. Pathways for degradation of plastic

polymers floating in the marine environment. Environmental Science-Processes & Impacts 17(9), 1513-1521. http://doi.org/ 10.1039/c5em00207a

Geyer, R., Jambeck, J.R. and Law, K.L., 2017. Production, use, and fate of all plastics ever made. Science Advances 3(7), e1700782. http://doi.org/ 10.1126/sciadv.1700782

Guo, X. and Wang, J., 2021. Projecting the sorption capacity of heavy metal ions onto microplastics in global aquatic environments using artificial neural networks. Journal of Hazardous Materials 402, 123709. http://doi.org/ 10.1016/j.jhazmat.2020.123709

Hamilton, B.M., Bourdages, M.P.T., Geoffroy, C., Vermaire, J.C., Mallory, M.L., Rochman, C.M. and Provencher, J.F., 2021. Microplastics around an Arctic seabird colony: Particle community composition varies across environmental matrices. Science of the Total Environment 773, 145536. http://doi.org/ 10.1016/j.scitotenv.2021.145536

Jahnke, A., Arp, H.P.H., Escher, B.I., Gewert, B., Gorokhova, E., Kuehnel, D., Ogonowski, M., Potthoff, A., Rummel, C., Schmitt-Jansen, M., Toorman, E. and MacLeod, M., 2017. Reducing Uncertainty and Confronting Ignorance about the Possible Impacts of Weathering Plastic in the Marine Environment. Environmental Science & Technology Letters 4(3), 85-90. http://doi.org/

Jeong, J. and Choi, J., 2019. Adverse outcome pathways potentially related to hazard identification of microplastics based on toxicity mechanisms. Chemosphere 231, 249-255. http://doi.org/ 10.1021/acs.estlett.7b00008

Jiang, X., Chang, Y., Zhang, T., Qiao, Y., Klobucar, G. and Li, M., 2020. Toxicological effects of polystyrene microplastics on earthworm (Eisenia fetida). Environmental Pollution 259, 113896. http://doi.org/ 10.1016/j.envpol.2019.113896

Kasal, A., Kuskun, T. and Smardzewski, J., 2020. Experimental and Numerical Study on Withdrawal Strength of Different Types of Auxetic Dowels for Furniture Joints. Materials 13(19),

4252. http://doi.org/ 10.3390/ma13194252

Khalid, N., Aqeel, M., Noman, A., 2020. Microplastics could be a threat to plants in terrestrial systems directly or indirectly. Environmental Pollution. 267, 115653. https://doi.org/10.1016/j.envpol.2020.115653.

Klasios, N., De Frond, H., Miller, E., Sedlak, M. and Rochman, C.M., 2021. Microplastics and other anthropogenic particles are prevalent in mussels from San Francisco Bay, and show no correlation with PAHs. Environmental Pollution 271, 116260. http://doi.org/ 10.1016/j.envpol.2020.116260

Kooi, M., Primpke, S., Mintenig, S.M., Lorenz, C., Gerdts, G. and Koelmans, A.A., 2021. Characterizing the multidimensionality of microplastics across environmental compartments. Water Research 202, 117429. http://doi.org/ 10.1016/j.watres.2021.117429

Kvale, K., Prowe, A.E.F., Chien, C.T., Landolfi, A. and Oschlies, A., 2021. Zooplankton grazing of microplastic can accelerate global loss of ocean oxygen. Nature Communications 12(1), 2358. 10.1038/s41467-021-22554-w

Lambert, S. and Wagner, M., 2016. Characterisation of nanoplastics during the degradation of polystyrene. Chemosphere 145, 265-268. http://doi.org/ 10.1016/j.chemosphere.2015.11.078

Leslie, H.A., van Velzen, M.J.M., Brandsma, S.H., Vethaak, A.D., Garcia-Vallejo, J.J. and Lamoree, M.H., 2022. Discovery and quantification of plastic particle pollution in human blood. Environment international 163, 107199-107199.

Li, H.M., Li, G.L., Hou, X.Q., Ma, X.P., Chen, J.T. and Kang, Z., 2018. Core melt temperature effects on cylindritic structures of co-injection molded polypropylene parts. International Communications in Heat and Mass Transfer 97, 56-63. http://doi.org/ 10.1016/j.icheatmasstransfer.2018.07.003

476 Li, Q., Zeng, A., Jiang, X. and Gu, X., 2021. Are microplastics correlated to phthalates in facility
477 agriculture soil? Journal of Hazardous Materials 412, 125164. http://doi.org/
478 10.1016/j.jhazmat.2021.125164
479 Li, W.J., Shao, L.Y., Wang, W.H., Li, H., Wang, X.M., Li, Y.W., Li, W.J., Jones, T. and Zhang,
480 D.Z., 2020a. Air quality improvement in response to intensified control strategies in Beijing during
481 2013-2019. Science of the Total Environment 744, 140776. http://doi.org/
482 10.1016/j.scitotenv.2020.140776
483 Li, Y.W., Shao, L.Y., Wang, W.H., Zhang, M.Y., Feng, X.L., Li, W.J. and Zhang, D.Z., 2020b.
484 Airborne fiber particles: Types, size and concentration observed in Beijing. Science of the Total
485 Environment 705, 135967. http://doi.org/ 10.1016/j.scitotenv.2019.135967
486 Liang, T., Lei, Z., Fuad, M.T.I., Wang, Q., Sun, S., Fang, J.K.-H. and Liu, X., 2022. Distribution
487 and potential sources of microplastics in sediments in remote lakes of Tibet, China. Science of the
488 Total Environment 806, 150526. http://doi.org/ 10.1016/j.scitotenv.2021.150526
489 Limonta, G., Mancia, A., Benkhalqui, A., Bertolucci, C., Abelli, L., Fossi, M.C. and Panti, C.,
490 2019. Microplastics induce transcriptional changes, immune response and behavioral alterations in
491 adult zebrafish. Scientific Reports 9, 15775. http://doi.org/ 10.1038/s41598-019-52292-5
492 Liu, G., Zhu, Z., Yang, Y., Sun, Y., Yu, F. and Ma, J., 2019a. Sorption behavior and mechanism
493 of hydrophilic organic chemicals to virgin and aged microplastics in freshwater and seawater.
494 Environmental Pollution 246, 26-33. http://doi.org/ 10.1016/j.envpol.2018.11.100
495 Liu, K., Wang, X., Fang, T., Xu, P., Zhu, L. and Li, D., 2019b. Source and potential risk
496 assessment of suspended atmospheric microplastics in Shanghai. Science of the Total Environment
497 675, 462-471. http://doi.org/ 10.1016/j.scitotenv.2019.04.110
498 Mao, R., Lang, M., Yu, X., Wu, R., Yang, X. and Guo, X., 2020. Aging mechanism of

499 microplastics with UV irradiation and its effects on the adsorption of heavy metals. Journal of
500 Hazardous Materials 393, 122515. http://doi.org/ 10.1016/j.jhazmat.2020.122515
501 Mohammadizadeh, M., Imeri, A., Fidan, I. and Elkelany, M., 2019. 3D printed fiber reinforced
502 polymer composites - Structural analysis. Composites Part B-Engineering 175, 107112.
503 http://doi.org/10.1016/j.compositesb.2019.107112
504 Moore, C.J., 2008. Synthetic polymers in the marine environment: A rapidly increasing, long-
505 term threat. Environmental Research 108(2), 131-139. http://doi.org/ 10.1016/j.envres.2008.07.025
506 Müller, A., Becker, R., Dorgerloh, U., Simon, F.-G. and Braun, U., 2018. The effect of polymer
507 aging on the uptake of fuel aromatics and ethers by microplastics. Environmental Pollution 240, 639-
508 646. http://doi.org/ 10.1016/j.envpol.2018.04.127
509 Murphy, F., Ewins, C., Carbonnier, F. and Quinn, B., 2016. Wastewater Treatment Works
510 (WwTW) as a Source of Microplastics in the Aquatic Environment. Environmental Science &
511 Technology 50(11), 5800-5808. http://doi.org/ 10.1021/acs.est.5b05416
512 Ng, E.L., Lin, S.Y., Dungan, A.M., Colwell, J.M., Ede, S., Lwanga, E.H., Meng, K., Geissen, V.,
513 Blackall, L.L. and Chen, D., 2021. Microplastic pollution alters forest soil microbiome. Journal of
514 Hazardous Materials 409, 124606. http://doi.org/ 10.1016/j.jhazmat.2020.124606
515 Parolini, M., Antonioli, D., Borgogno, F., Gibellino, M.C., Cavallo, R.J.I.J.o.E.R. and Health, P.,
516 2021. Microplastic Contamination in Snow from Western Italian Alps. International Journal of
517 Environmental Research And Public Health 18(2), 768. http://doi.org/ 10.3390/ijerph18020768
518 Pastorino, P., Nocita, A., Ciccotelli, V., Zaccaroni, A., Anselmi, S., Giugliano, R., Tomasoni, M.,
519 Silvi, M., Menconi, V., Vivaldi, B., Pizzul, E., Renzi, M. and Prearo, M., 2021. Health risk assessment
520 of potentially toxic elements, persistence of NDL-PCB, PAHS, and microplastics in the translocated
521 edible freshwater sinotaia quadrata (gasteropoda, viviparidae): A case study from the arno river basin

(central italy). Exposure and Health 14, 583-896. http://doi.org/ 10.1007/s12403-021-00404-w

Prata, J.C., da Costa, J.P., Lopes, I., Duarte, A.C. and Rocha-Santos, T., 2020. Environmental exposure to microplastics: An overview on possible human health effects. Science of the Total Environment 702, 134455. http://doi.org/ 10.1016/j.scitotenv.2019.134455

Qiao, R., Sheng, C., Lu, Y., Zhang, Y., Ren, H. and Lemos, B., 2019. Microplastics induce intestinal inflammation, oxidative stress, and disorders of metabolome and microbiome in zebrafish. Science of the Total Environment 662, 246-253. http://doi.org/ 10.1016/j.scitotenv.2019.01.245

Ren, Z., Gui, X., Xu, X., Zhao, L., Qiu, H. and Cao, X., 2021. Microplastics in the soil-groundwater environment: Aging, migration, and co-transport of contaminants-A critical review. Journal of Hazardous Materials 419, 126455. http://doi.org/ 10.1016/j.jhazmat.2021.126455

Revell, L.E., Kuma, P., Le Ru, E.C., Somerville, W.R.C. and Gaw, S., 2021. Direct radiative effects of airborne microplastics. Nature 598(7881), 462-467. http://doi.org/ 10.1038/s41586-021-03864-x

Saarni, S., Hartikainen, S., Meronen, S., Uurasjarvi, E., Kalliokoski, M. and Koistinen, A., 2021. Sediment trapping - An attempt to monitor temporal variation of microplastic flux rates in aquatic systems. Environmental Pollution 274, 116568. http://doi.org/ 10.1016/j.envpol.2021.116568

Salimi, A., Alavehzadeh, A., Ramezani, M. and Pourahmad, J., 2022. Differences in sensitivity of human lymphocytes and fish lymphocytes to polyvinyl chloride microplastic toxicity. Toxicology and Industrial Health 38(2), 100-111. https://doi.org/10.1177/07482337211065832.

Serranti, S., Palmieri, R., Bonifazi, G. and Cozar, A., 2018. Characterization of microplastic litter from oceans by an innovative approach based on hyperspectral imaging. Waste Management 76, 117-125. http://doi.org/ 10.1016/j.wasman.2018.03.003

Shao, L.Y., Li, J., Zhang, M.Y., Wang, X., Li, Y.W., Jones, T., Feng, X.L., Silva, L.F.O. and Li,

W.J., 2021a. Morphology, composition and mixing state of individual airborne particles: Effects of the 2017 Action Plan in Beijing, China. Journal of Cleaner Production 329, 129748. http://doi.org/ 10.1016/j.jclepro.2021.129748

Shao, L.Y., Ge, S.Y., Jones, T., Santosh, M., Silva, L.F.O., Cao, Y.X., Oliveira, M.L.S., Zhang, M.Y. and BeruBe, K., 2021b. The role of airborne particles and environmental considerations in the transmission of SARS-CoV-2. Geoscience Frontiers 12(5), 101189. https://doi.org/10.1016/j.gsf.2021.101189.

Shao, L.Y., Li, Y.W., Jones, T., Santosh, M., Liu, P.J., Zhang, M.Y., Xu, L., Li, W.J., Lu, J., Yang, C.-X., Zhang, D.Z., Feng, X.L., and BéruBé, K., 2022a. Airborne microplastics: A review of current perspectives and environmental implications. Journal of Cleaner Production 347, 131048. http://doi.org/ 10.1016/j.jclepro.2022.131048

Shao, L.Y ., Liu, P.J., Jones, T., Yang, S.S., Wang, W.H., Zhang, D.Z., Li, Y.W., Yang, C.-X., Xing, J.P., Hou, C., Zhang, M.Y., Feng, X.L., Li, W.J. and BéruBé, K., 2022b. A review of atmospheric individual particle analyses: Methodologies and applications in environmental research. Gondwana Research. http://doi.org/ 10.1016/j.gr.2022.01.007

Halle, A., Ladirat, L., Martignac, M., Mingotaud, A.F., Boyron, O. and Perez, E., 2017. To what extent are microplastics from the open ocean weathered? Environmental Pollution 227, 167-174. http://doi.org/ 10.1016/j.envpol.2017.04.051

Van Cauwenberghe, L. and Janssen, C.R., 2014. Microplastics in bivalves cultured for human consumption. Environmental Pollution 193, 65-70. http://doi.org/ 10.1016/j.envpol.2014.06.010

Vermeiren, P., Lercari, D., Munoz, C.C., Ikejima, K., Celentano, E., Jorge-Romero, G. and Defeo, O., 2021. Sediment grain size determines microplastic exposure landscapes for sandy beach macroinfaunak. Environmental Pollution 286, 117308. http://doi.org/ 10.1016/j.envpol.2021.117308

568 Wang, J., Peng, C., Li, H., Zhang, P. and Liu, X., 2021. The impact of microplastic-microbe
569 interactions on animal health and biogeochemical cycles: A mini-review. Science of the Total
570 Environment 773, 145697. http://doi.org/ 10.1016/j.scitotenv.2021.145697
571 Wang, W., Gao, H., Jin, S., Li, R. and Na, G., 2019. The ecotoxicological effects of microplastics
572 on aquatic food web, from primary producer to human: A review. Ecotoxicology and Environmental
573 Safety 173, 110-117. http://doi.org/ 10.1016/j.ecoenv.2019.01.113
574 Wang, W.H., Shao, L.Y., Zhang, D.Z., Li, Y.W., Li, W.J., Liu, P.J. and Xing, J.P., 2022.
575 Mineralogical similarities and differences of dust storm particles at Beijing from deserts in the north
576 and northwest. Science of the Total Environment 803, 149980. http://doi.org/
577 10.1016/j.scitotenv.2021.149980
578 Ward, J.E. and Kach, D.J., 2009. Marine aggregates facilitate ingestion of nanoparticles by
579 suspension-feeding bivalves. Marine Environmental Research 68(3), 137-142. http://doi.org/
580 10.1016/j.marenvres.2009.05.002
581 Welle, F., Bayer, F. and Franz, R., 2012. Quantification of the Sorption Behavior of Polyethylene
582 Terephthalate Polymer versus PET/PA Polymer Blends towards Organic Compounds. Packaging
583 Technology and Science 25(6), 341-349. http://doi.org/ 10.1002/pts.984
584 Woodward, J., Li, J.W., Rothwell, J. and Hurley, R., 2021. Acute riverine microplastic
585 contamination due to avoidable releases of untreated wastewater. Nature Sustainability 4(9), 793-+.
586 http://doi.org/ 10.1038/s41893-021-00718-2
587 Yan, Z., Chen, Y., Bao, X., Zhang, X., Ling, X., Lu, G., Liu, J. and Nie, Y., 2021. Microplastic
588 pollution in an urbanized river affected by water diversion: Combining with active biomonitoring.
589 Journal of Hazardous Materials 417, 126058. http://doi.org/ 10.1016/j.jhazmat.2021.126058
590 Yang, L., Luo, W., Zhao, P., Zhang, Y. and Zhang, F.J.E.P., 2021. Microplastics in the Koshi

591 River, a remote alpine river crossing the Himalayas from China to Nepal. Environmental Pollution
592 290, 118121. http://doi.org/ 10.1016/j.envpol.2021.118121
593 Zhang, C., Lei, Y., Qian, J., Qiao, Y., Liu, J., Li, S., Dai, L., Sun, K., Guo, H., Sui, G. and Jing,
594 W., 2021a. Sorption of organochlorine pesticides on polyethylene microplastics in soil suspension.
595 Ecotoxicology and Environmental Safety 223, 112591. http://doi.org/ 10.1016/j.ecoenv.2021.112591
596 Zhang, C., Wang, J., Zhou, A., Ye, Q., Feng, Y., Wang, Z., Wang, S., Xu, G. and Zou, J., 2021b.
597 Species-specific effect of microplastics on fish embryos and observation of toxicity kinetics in larvae.
598 Journal of Hazardous Materials 403, 123948. http://doi.org/ 10.1016/j.jhazmat.2020.123948
599 Zhang, K., Su, J., Xiong, X., Wu, X., Wu, C. and Liu, J., 2016. Microplastic pollution of
600 lakeshore sediments from remote lakes in Tibet plateau, China. Environmental Pollution 219, 450-
601 455. http://doi.org/ 10.1016/j.envpol.2016.05.048
602 Zhou, Z., Zhang, P., Zhang, G., Wang, S., Cai, Y. and Wang, H., 2021. Vertical microplastic
603 distribution in sediments of Fuhe River estuary to Baiyangdian Wetland in Northern China.
604 Chemosphere 280, 130800. http://doi.org/ 10.1016/j.chemosphere.2021.130800
605

606 **Table caption**

607 Table 1. The details of sample collection in Beijing.

608

609

610 **Figure captions**

611 Fig. 1. Location of the study area and distribution of the sampling sites.

612

613 Fig. 2. The number concentrations of MPs at the different sampling sites in the Beijing dustfall.

614

615 Fig. 3. Wavenumber and absorbance of different compositional types of microplastics collected in
616 Beijing dustfall. The solid line is the spectrum obtained by particle testing, and the dotted line is the
617 standard spectrum.

618

619 Fig. 4. The number concentrations of different compositional types of MPs in the Beijing dustfall.
620 Polypropylene (PP), Polyamide (PA), Polystyrene (PS), Polyethylene (PE), Polyethylene
621 Terephthalate (PET), Silicone, Polycarbonate (PC), Polyurethane (PU) and Polyvinylchloride (PVC).

622

623 Fig. 5. Relative abundances of different compositional types of MPs at different sampling sites in the
624 Beijing fallout dust. Polypropylene (PP), Polyamide (PA), Polystyrene (PS), Polyethylene (PE),
625 Polyethylene Terephthalate (PET), Silicone, Polycarbonate (PC), Polyurethane (PU) and
626 Polyvinylchloride (PVC).

627

628 Fig. 6. FESEM images showing different morphological types of MPS in the Beijing dustfall. a,
629 pellet/sphere; b, fragment; c and d, fiber; e, higher magnification of a stress embrittlement on the fiber
630 in image d.

631

632 Fig. 7. The relative abundances of different MPs morphological types at different sampling sites in
633 the Beijing dustfall.

634

635 Fig. 8. The relative abundances of different MPs morphological types for the different compositional
636 types in the Beijing dustfall.

637

638 Fig. 9. Averaged sizes by equivalent circular diameter of the different MPs in the Beijing dustfall.
639 The error bar stands for the standard deviation.

640

641 Fig. 10. The number of microplastics in different MPs size ranges in the Beijing dustfall.

642

643 Fig. 11. Relative abundance of different morphological types in different MPs size ranges in the
644 Beijing dustfall.

645

646 Fig. 12. Relative abundance of pellets, fragments, and fibers in different size ranges of MPs in the
647 Beijing dustfall.

648

649

650

651 Table 1. The details of sample collection in Beijing.

Sample No	Sampling day	Sampling site environment	Wind direction
S1	2021.06.09	Residential area	North wind
S2		Park	
S3		Near the road (There are tall buildings between the sampling site and the road)	
S4	2021.06.10	Under the office building	West wind
S5	2021.12.10	Nanluoguxiang (residential areas, food stalls street, densely populated)	North wind
S6	2021.06.10	Residential area (close to tourism service industry)	West wind
S7	2021.12.11	Near the road (there are tall buildings between the sampling site and the road)	Northwest wind
S8	2021.06.10	Residential area (close to a pharmaceutical company)	West wind
S9	2021.06.15	Outside the residential area (close to construction activity)	North wind
S10		Residential area (close to beverage, furniture, machinery, and clothing companies)	

652

653

654

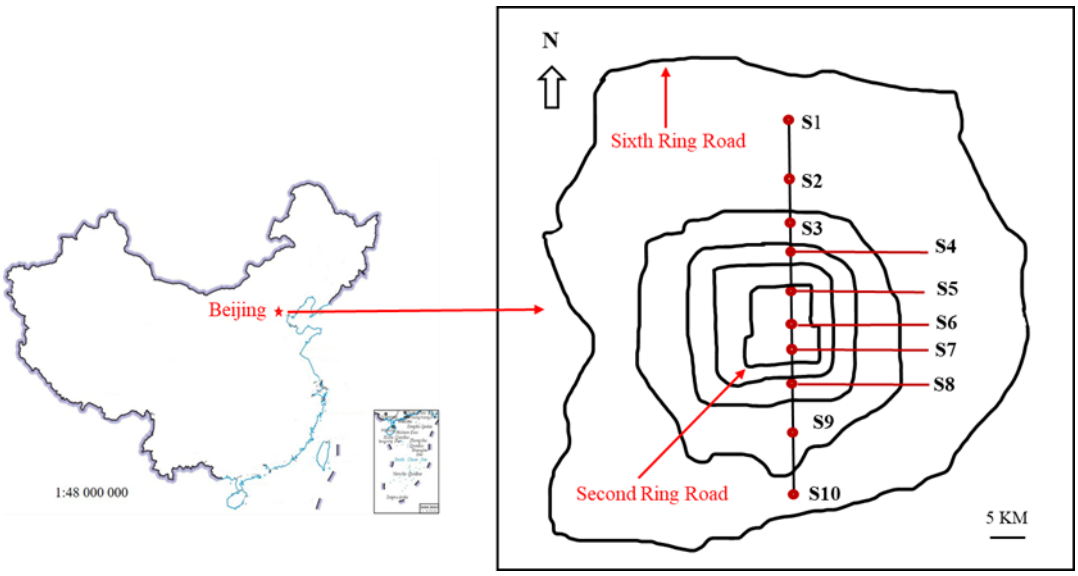

Fig. 1. Location of the study area and distribution of the sampling sites.

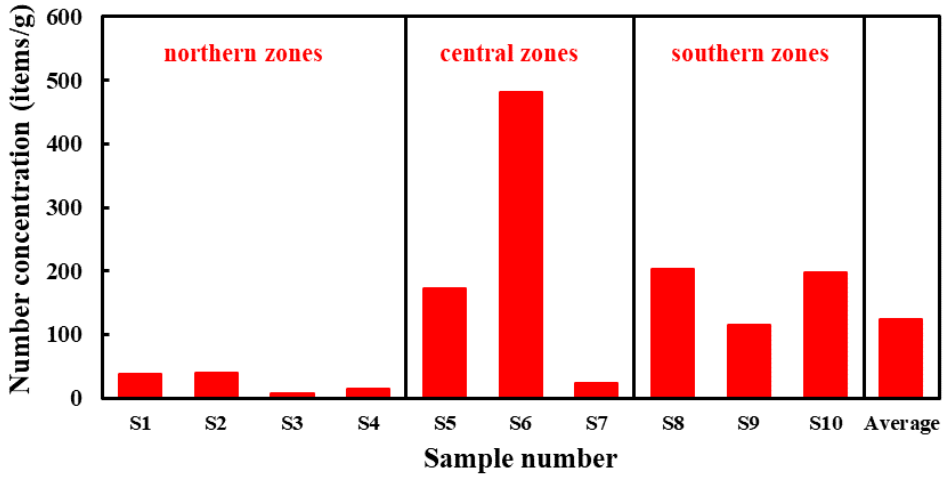

Fig. 2. The number concentrations of MPs at the different sampling sites in the Beijing dustfall.

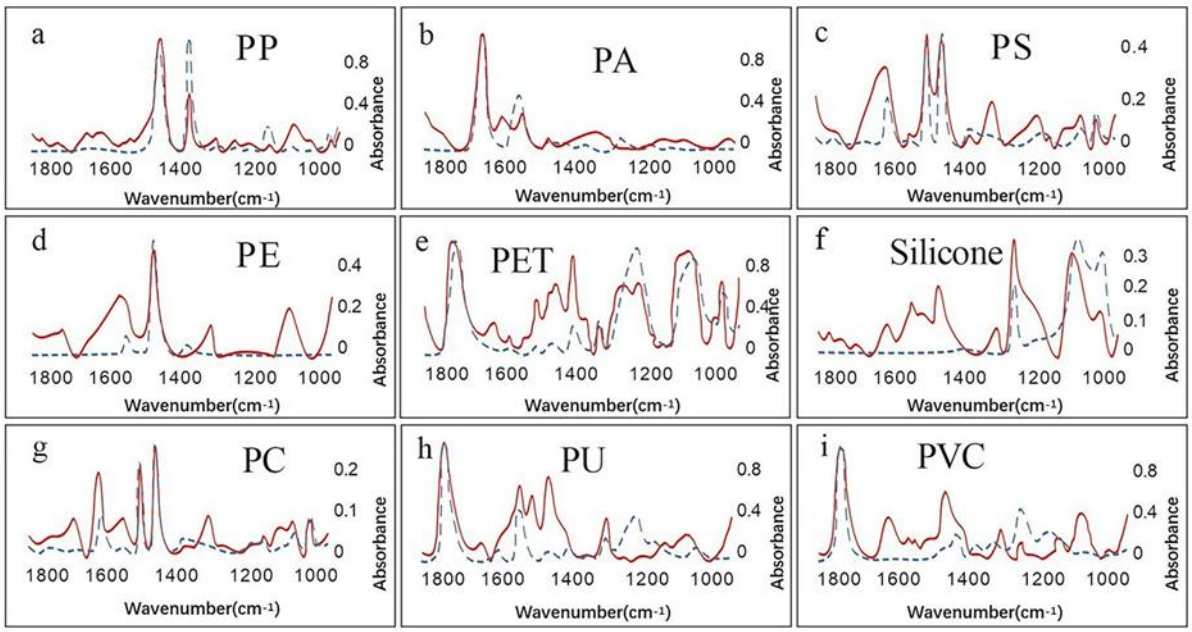

660

661 Fig. 3. Wavenumber and absorbance of different compositional types of microplastics collected in

662 Beijing dustfall. The solid line is the spectrum obtained by particle testing, and the dotted line is the

663 standard spectrum.

664

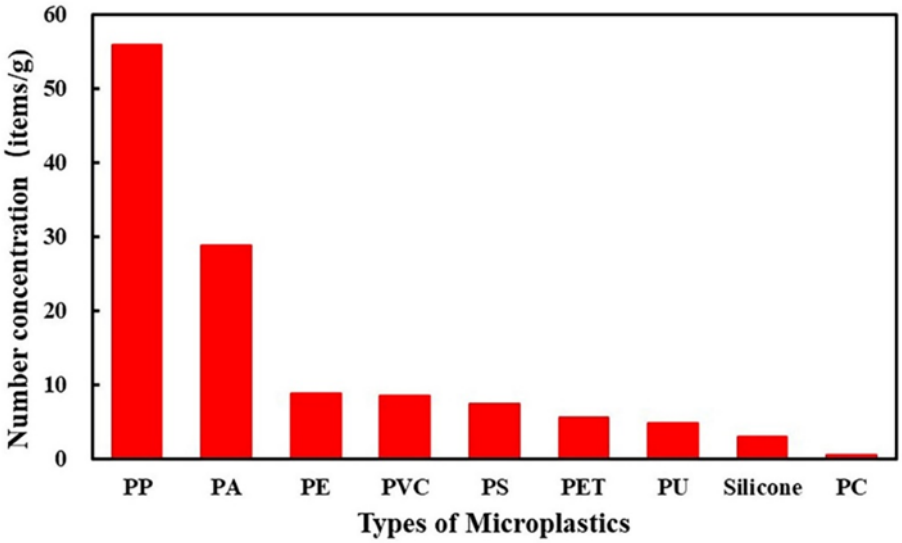

665

666 Fig. 4. The number concentrations of different compositional types of MPs in the Beijing dustfall.

667 Polypropylene (PP), Polyamide (PA), Polystyrene (PS), Polyethylene (PE), Polyethylene

668 Terephthalate (PET), Silicone, Polycarbonate (PC), Polyurethane (PU) and Polyvinylchloride (PVC).

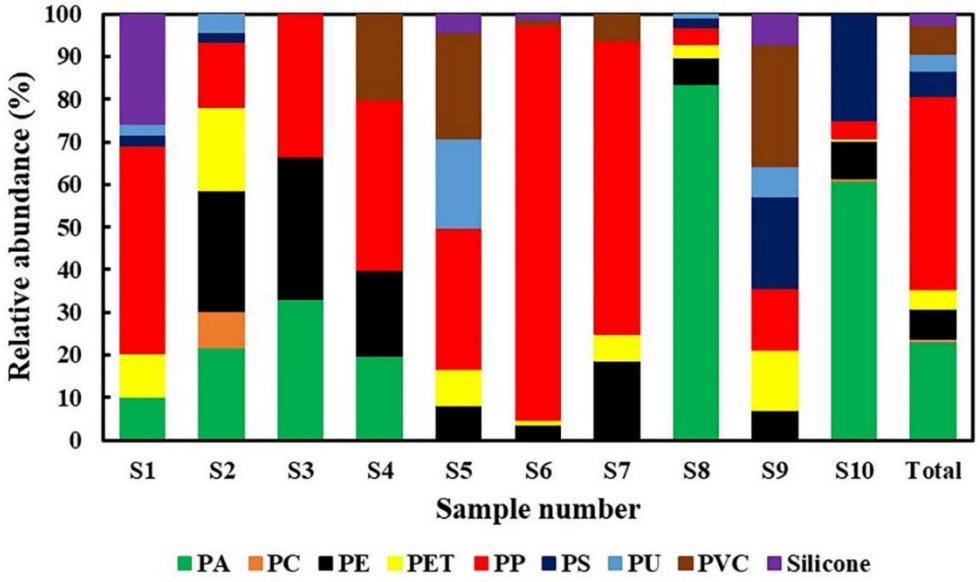

669

670 Fig. 5. Relative abundances of different compositional types of MPs at different sampling sites in the
671 Beijing fallout dust. Polypropylene (PP), Polyamide (PA), Polystyrene (PS), Polyethylene (PE),
672 Polyethylene Terephthalate (PET), Silicone, Polycarbonate (PC), Polyurethane (PU) and
673 Polyvinylchloride (PVC).

674

675

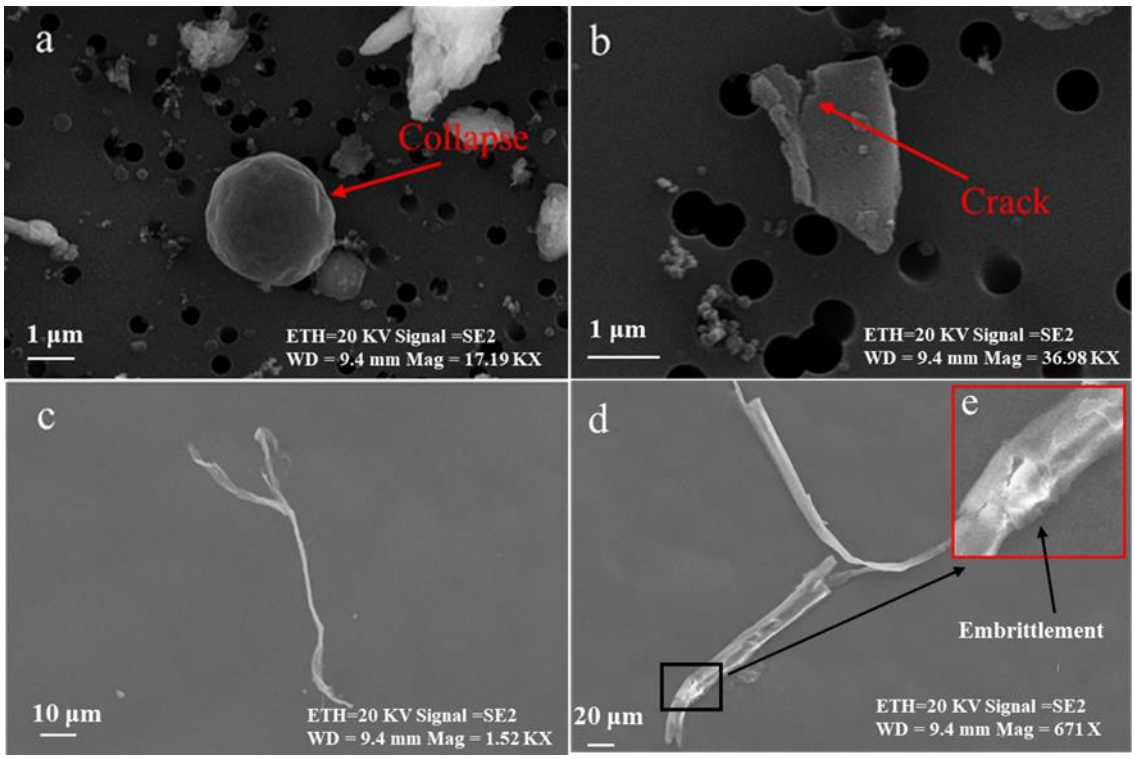

Fig. 6. FESEM images showing different morphological types of MPS in the Beijing dustfall. a, pellet/sphere; b, fragment; c and d, fiber; e, higher magnification of a stress embrittlement on the fiber in image d.

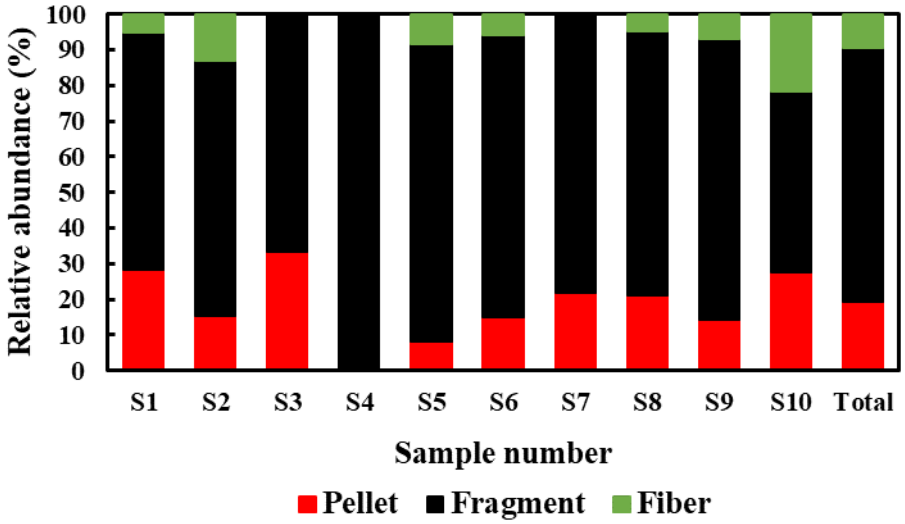

Fig. 7. The relative abundances of different MPs morphological types at different sampling sites in the Beijing dustfall.

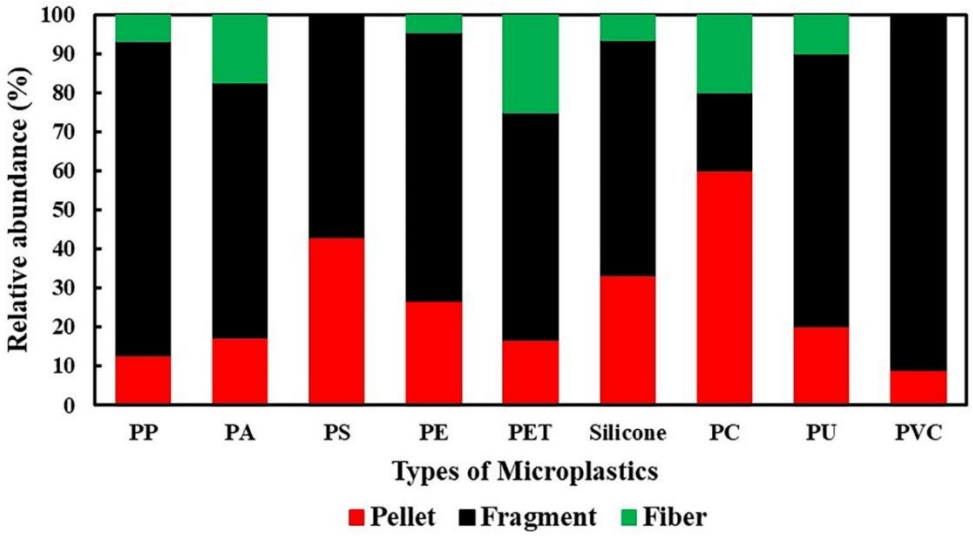

Fig. 8. The relative abundances of different MPs morphological types for the different compositional types in the Beijing dustfall.

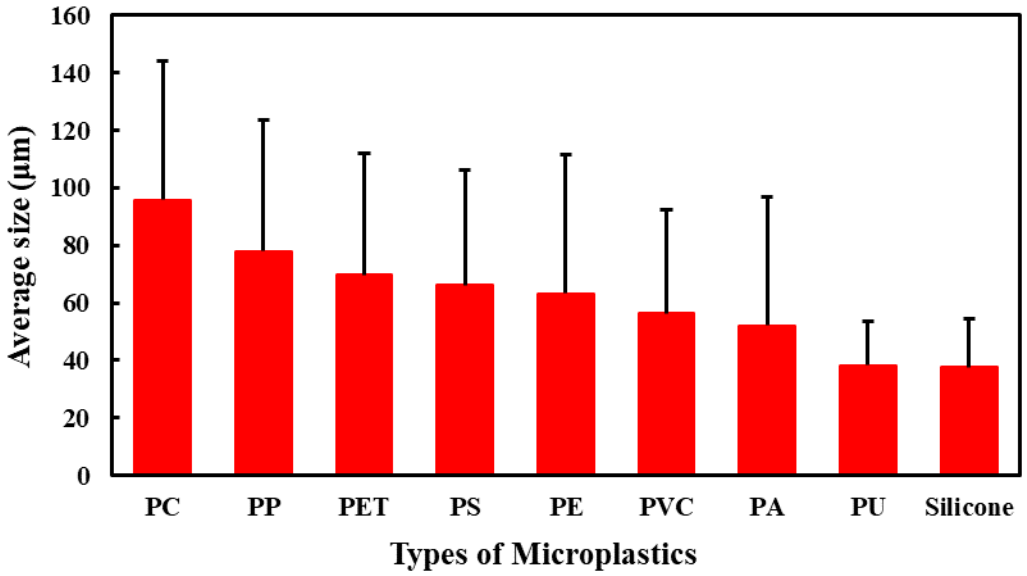

Fig. 9. Averaged sizes by equivalent circular diameter of the different MPs in the Beijing dustfall. The error bar stands for the standard deviation.

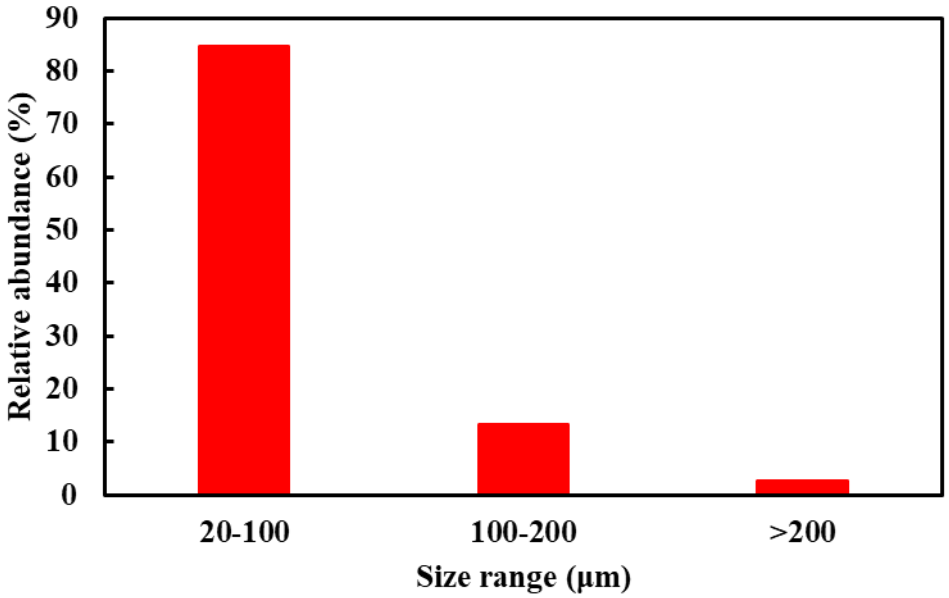

Fig. 10. The number of microplastics in different MPs size ranges in the Beijing dustfall.

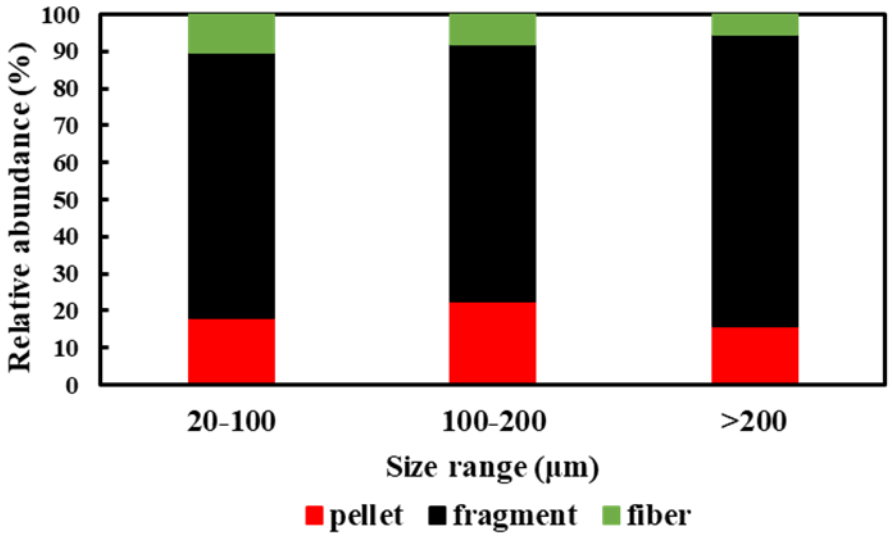

Fig. 11. Relative abundance of different morphological types in different MPs size ranges in the Beijing dustfall.

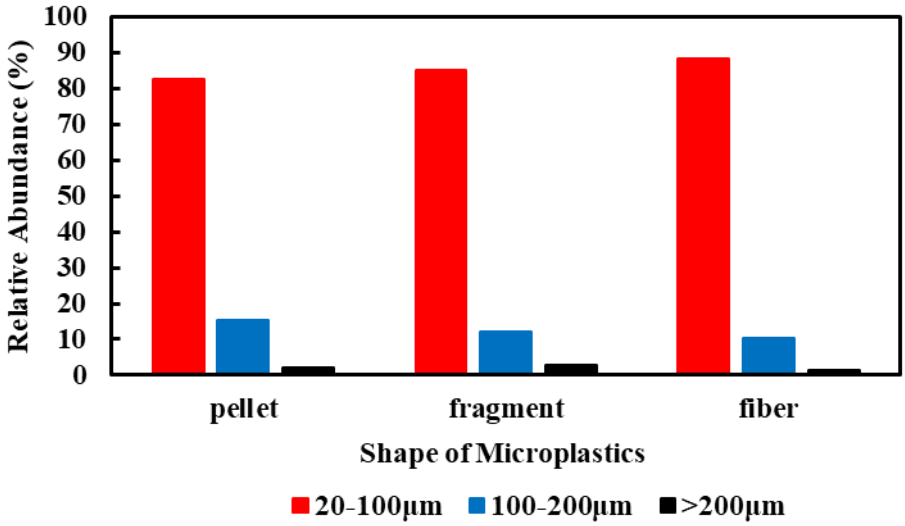

Fig. 12. Relative abundance of pellets, fragments, and fibers in different size ranges of MPs in the Beijing dustfall.